Energy 179 (2019) 1205–1216

Contents lists available at ScienceDirect

Energy

journal homepage: www.elsevier.com/locate/energy

Carbon and sulfur conversion of petroleum coke in the chemical looping gasification process

Lulu Wang [a], Xuan Feng [a], Laihong Shen [a, *], Shouxi Jiang [a], Haiming Gu [b]

[a] Key Laboratory of Energy Thermal Conversion and Control of Ministry of Education, School of Energy and Environment, Southeast University, Nanjing, 210096, China
[b] School of Energy and Power Engineering, Nanjing Institute of Technology, China

ARTICLE INFO

Article history:
Received 2 December 2018
Received in revised form
16 March 2019
Accepted 18 April 2019
Available online 3 May 2019

Keywords:
Chemical looping gasification
Petroleum coke
Hematite
Sulfur recovery
Claus process

ABSTRACT

Petroleum coke is the waste from the delay coking process during petroleum refining. It is urgent to solve the problem of the effective and environmental utilization of high-sulfur petroleum coke. Chemical looping gasification (CLG) is employed in the application of petroleum coke for syngas production and sulfur recovery for the first time. The conventional steam gasification was for comparison to have a better understanding of the chemical looping process of petroleum coke. The presence of hematite improved the carbon conversion efficiency to 70.13%, although the fraction of the effective syngas decreased slightly. Experiments are conducted to evaluate the effects of temperature, steam flow rate and the sizes of fuel and hematite on the conversion of carbon and sulfur in a batch fluidized bed. The data shows that the effective syngas accounts for 83.51% and the molar fraction of H_2S/SO_2 is about 2, when the fuel size was 0.1–0.3 mm, and the hematite size was 0.3–0.4 mm at the steam flow rate of 1 g/min at 900 °C. Moreover, that condition is advantageous to the further utilization of the flue gas stream for sulfur recovery via Claus process. The size of oxygen carrier has a significant influence on distribution of sulfur species releasing. The high-content sulfur in the petroleum coke did not remain on the surface of hematite and the oxygen carriers were not poisoned. As a consequence, chemical looping gasification with hematite as oxygen carrier is an excellent technique for petroleum coke conversion coupled with sulfur recovery.

1. Introduction

Petroleum coke is the waste from the delayed coking process in the petroleum refining industry with high calorific value and low ash content. It is classified to high and low sulfur petroleum coke depending on the sulfur content. The low sulfur one can be used in many fields such as fuel, anode and electrode. However, the high sulfur petroleum coke faces a great challenge to be utilized because of the pollution [1,2]. Moreover, the production yield of high sulfur coke is overstocked with a high increasing rate, while the low sulfur one is in short supply [3]. Therefore, the utilization of high sulfur petroleum coke in a benign environmental and effective method is being solved urgently [4].

Gasification is considered as a cleaner and economic process to convert solid fuels in comparison with combustion [5–7]. When petroleum coke is used in the gasification technology, the sulfur compounds in the raw gas product would be converted into elemental sulfur in the Claus plant. But the gasification reactivity of petroleum coke is rather low due to its carbon structure and low combustibility [8,9]. Chemical looping gasification (CLG) is a promising gasification technology to produce syngas, sharing the same principle with chemical looping combustion (CLC) [10]. Generally, the system involves two reactors, a fuel reactor and an air reactor, with the oxygen carrier circulating between the two reactors as shown in Fig. 1. The oxygen carrier transfers lattice oxygen and heat to achieve the fuel partial oxidation and gasification in the fuel reactor, while the reductive oxygen carrier is transported for regeneration in the air reactor.

Compared with the traditional gasification technology, CLG has several advantages [11,12]. The regeneration of oxygen carrier can supply heat for gasification, thus balancing the heat in the system with less extra energy input. The oxygen carrier provides lattice oxygen in order to reduce the costs associated with pure O_2 requirement which is the main expenditure for the traditional

* Corresponding author.
E-mail address: lhshen@seu.edu.cn (L. Shen).

https://doi.org/10.1016/j.energy.2019.04.109
0360-5442/

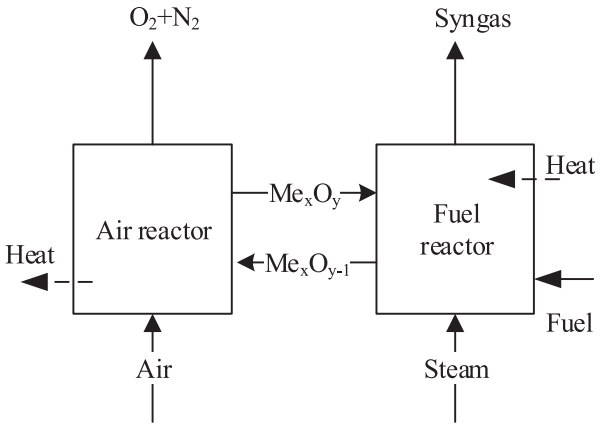

Fig. 1. Schematic diagram of chemical looping gasification process.

gasification. For traditional gasification, many kinds of catalysts were used to improve the gasification rate, but the catalyst cannot be recycled [4,13,14]. The recycled oxygen carrier is also considered as catalyst which improves the gasification reactions and has an excellent reactivity at a lower reaction temperature.

Currently, CLG is widely used to deal with solid fuels such as coal and biomass [11,12,15–19]. Guo et al. [11] have found that the carbon conversion efficiency of coal increased by 25.26% with increasing O/C ratio, and indicated that the reactions in the CLG would include three stages: the gasification of coal char; the complex CLC reactions involving oxygen carrier, coal char, and steam; and the reduction of Fe_3O_4 to FeO. Huang et al. [17] claimed that the lattice oxygen from oxygen carrier played the similar role as gasification agent for biomass gasification, but the reactivity of lattice oxygen was lower than steam. Additionally, the adequate and stable oxygen carrier is the key to the development of chemical looping process. Metal oxides are always supported by inert materials with high melting temperature such as SiO_2, Al_2O_3 or ZrO_2 synthetically to improve the lifetime, and stability of oxygen carrier significantly [20–22]. Among the different types of materials, Fe-based oxygen carrier have been examined as the proper one for CLG process [11,18,23]. Additionally, Fe-based compounds are considered as attractive catalysts for gasification of petroleum coke [4]. In particular, iron ore is a potential natural oxygen carrier to reduce the cost of manufacturing. It composes of active phase (Fe_2O_3) and inert materials (SiO_2 and Al_2O_3) which can inhibit sintering and improve the durability of oxygen carrier [24]. With the advantages of sufficient source, low cost and non-toxicity, iron ore is suitable to use in large-scale system for CLG process despite the fact of its poor oxygen transport capacity.

It was noted that the researches always focused on the solid fuel of good reactivity. But the low price, abundant supply, high calorific value and low ash content make petroleum coke to be an attractive fuel as well. Nevertheless, there is few work on the CLG based on petroleum coke. It is the first time to utilize petroleum coke for syngas production and sulfur recovery via the CLG process. It is necessary to investigate the feasibility of the utilization of petroleum coke by chemical looping gasification. The work focuses on the effects of the presence of hematite, reaction temperature, steam concentration, and the size of hematite and petroleum coke on the fuel conversion in the batch fluidized bed. The property of sulfur conversion was first studied as well. Furthermore, we tried to find out the optimum condition for sulfur recovery via Claus reaction. The characteristics of oxygen carriers were also evaluated.

2. Experimental

2.1. Materials

Natural Australia hematite, provided by Nanjing Steel Manufacturing Company, is selected as oxygen carrier. Before using, it was crushed and sieved into particles ranging from 0.1 to 0.2 mm, 0.2–0.3 mm, 0.3–0.4 mm. And the particles were calcined in a muffle oven for 3 h at 950 °C. The chemical composition of hematite was based on the X-ray Fluorescence (XRF) analysis. The Brunauer-Emmett-Teller (BET) surface area of the particles in the size of 0.2–0.3 mm was also measured, and the mechanical strength was measured by FGJ-15 dynamometer. The results are summarized in Table 1. The high content of Al_2O_3 and SiO_2 in the hematite can be considered as the inert carrier to inhibit sintering, improve heating transform and stabilize the reactivity [24]. Quartz sand was selected as the inert bed material for blank experiments because of the excellent mechanical performance and heat transmission. The size range of quartz sand was 0.2–0.3 mm, and the bulk density was 1.5×10^3 kg/m^3.

Petroleum coke supplied by Yangzi Petrochemical International Trading Company is used as fuel. Prior to the experiments, the petroleum coke was pulverized and sieved to get the particles in the size range of 0.1–0.3 mm, 0.3–0.45 mm, 0.45–0.6 mm. The size ranges of fuel are different from hematite to separate the unreacted fuel and used oxygen carrier easily. The size of petroleum coke is bigger than that of hematite, because the density of fuel is lower. The scanning electron microscope (SEM) image of petroleum coke was shown in Fig. 2, and that of lignite coal is for comparison. The surface of petroleum coke was dense without obvious opening pores, while some cracks were observed on the coal surface. This can explain why the reactivity of petroleum coke is weak [25]. The respective proximate and ultimate analysis of petroleum coke were summarized in Table 2.

2.2. Experimental apparatus and procedure

Tests are conducted in a laboratory-scale batch fluidized bed, as illustrated in Fig. 3(a). The same system was frequently used in the earlier studies on chemical looping based on variety of oxygen carriers [26–31]. The major part is a reactor tube made of quartz, whose length is 600 mm and inner diameter is 32 mm. The system is heated by ovens. A porous distributor plate is installed in the middle of the tube. It makes the inlet gas smooth and steady and is also considered as the support of bed materials. There are two K-type thermocouples to control the reaction temperature: one is between the refractory insulating layer and reactor; another is above the distributor plate in the central axis of the reactor. N_2, O_2 and steam are injected from the bottom of tube as the fluidizing

Table 1
Properties of the natural hematite oxygen carrier.

	Natural Hematite
Chemical composition (wt.%)	
Fe_2O_3	83.21
Al_2O_3	5.35
SiO_2	7.06
MgO	1.92
TiO_2	0.1
P_2O_5	0.38
CaO	0.23
others	1.75
BET surface area (m^2/g)	2.96
Bulk density (kg/m^3)	1.7
Mechanical strength (N)	3.2

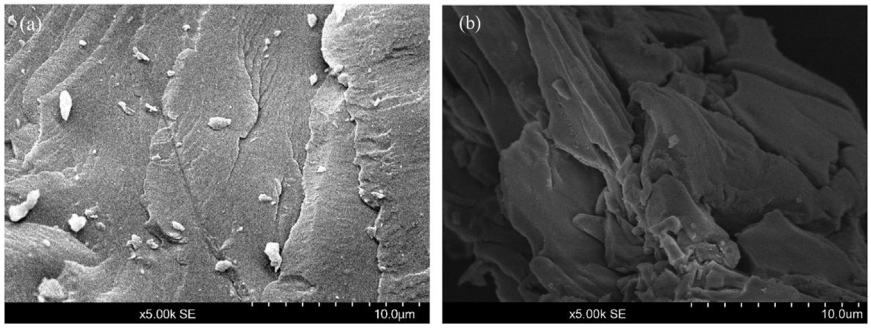

Fig. 2. SEM images of petroleum coke and lignite coal.

Table 2
Proximate and ultimate analysis of petroleum coke.

	Proximate analysis (wt.%, ad)				Ultimate analysis (wt.%, ad)				
	M	V	FC	A	C	H	O	N	S
Petroleum coke	0.76	12.98	85.87	0.39	85.94	3.24	1.92	0.94	6.81

gas, oxidizing agent and gasification agent, respectively. The steam generator is composed of a TBP-50 A type constant flow pump and a heater, and the steam flow is controlled precisely by adjusting the mass flow of deionized water.

Experimental flowchart is displayed in Fig. 3(b). In the batch tests, samples of bed materials with 36 g hematite are added into the reactor by the chute and placed on the distributor place when it reaches the desired reaction temperature at the atmosphere of N_2 (2 L/min STP). The amount of bed materials is guaranteed to maintain the same bed height after adding into the tube. Next, the oxygen carrier is exposed in a mixture of O_2 (100 ml/min STP) and N_2 atmosphere, which could ensure the natural hematite fully oxidized before the petroleum coke is introduced. H_2O preheated at 180 °C is injected to the bottom of the fluidized bed as gasification agent together with N_2 (1 L/min STP). Subsequently, petroleum coke (0.75 g) is fed from the reservoir at the top of the reactor, and the fuel is quickly introduced into the reaction zone by a valve. As soon as the fuel particles fall in the reactor, the coke has an intensive contact with the fresh oxygen carrier. The gaseous product was collected by gas bags after a filter, a cooler and a drier for offline analysis of H_2, CO_2, CO, and CH_4 by a NGA2000 type gas analyzer (EMERSON Company, USA). When the conversion of sulfur was evaluated, the experiment was repeated and N_2 (5 L/min STP) was injected in the exhaust gas to dilute the concentration of H_2S and SO_2. The gas flowed through a heating line of 120 °C and was measured online by a VARIO PLUS type gas analyzer (MRU, Germany). All the investigated cases are shown in Table 3. The uncertainties of the instruments mentioned are shown in Table 4. To ensure the validity of experimental results, six identical experiments were conducted under the same condition, three of which were used to analyze conventional gases (H_2, CO_2, CO, and CH_4) and three to detect the release of sulfur-containing gases (H_2S and SO_2).

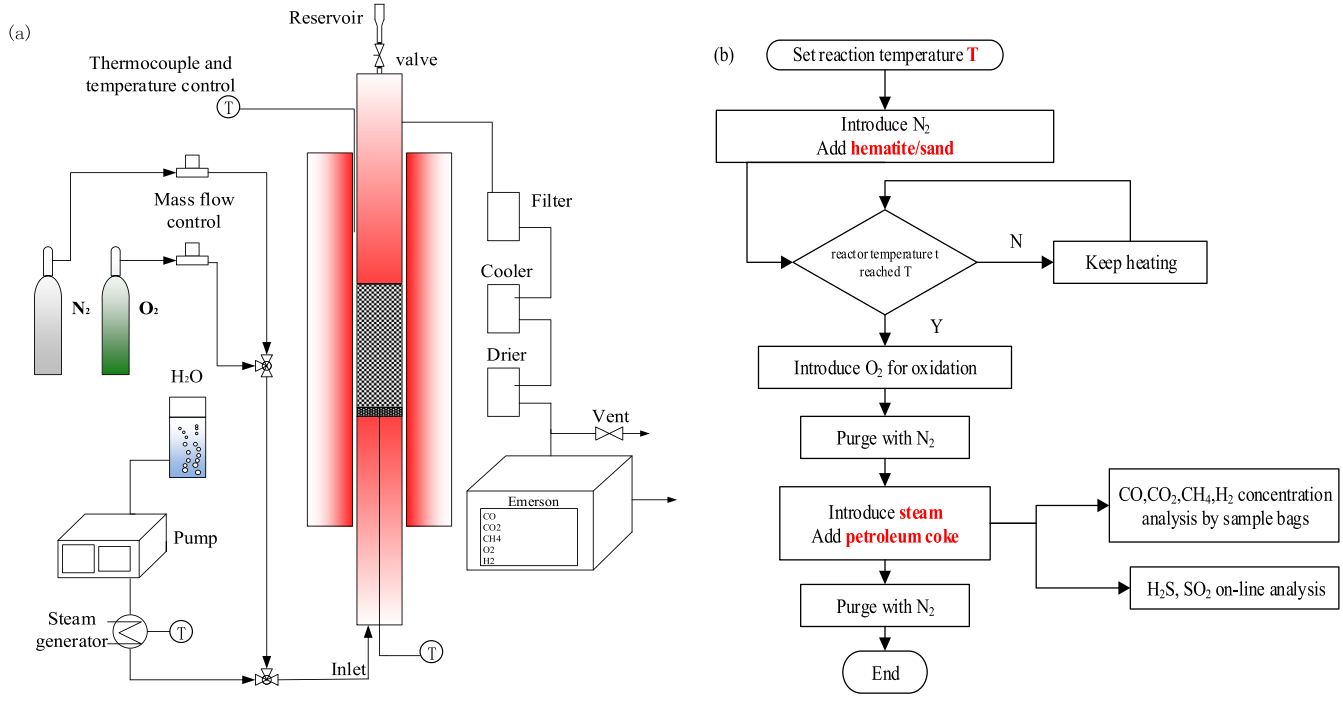

Fig. 3. Schematic layout of the laboratory setup (a) and experimental flowchart (b).

Table 3
All investigated cases.

Experimental process	Bed material	Particle size (mm)	Steam flow rate (g/min)	Temperature (°C)	Fuel size (mm)
Steam gasification	Quartz sand	0.2–0.3	1.0	900	0.1–0.3
CLG	Iron ore	0.2–0.3	1.0	900	0.1–0.3
CLG	Iron ore	0.2–0.3	1.0	850	0.1–0.3
CLG	Iron ore	0.2–0.3	1.0	950	0.1–0.3
CLG	Iron ore	0.2–0.3	0.5	900	0.1–0.3
CLG	Iron ore	0.2–0.3	1.5	900	0.1–0.3
CLG	Iron ore	0.2–0.3	1.0	900	0.3–0.45
CLG	Iron ore	0.2–0.3	1.0	900	0.45–0.6
CLG	Iron ore	0.1–0.2	1.0	900	0.1–0.3
CLG	Iron ore	0.3–0.4	1.0	900	0.1–0.3

Table 4
Uncertainty analysis.

Parameters	control temperature	N_2 flow	steam flow	CO	H_2S	H_2
uncertainty	±1 °C	±0.1 L/min	±0.01 g/min	±0.01%	±5 ppm	±0.1%
parameters	test temperature	O_2 flow	CO_2	CH_4	SO_2	
uncertainty	±1 °C	±0.005 L/min	±0.01%	±0.01%	±5 ppm	

2.3. Data evaluation

The inlet molar flow rate of N_2, f_{N_2}, is settled and the outlet gas (CO, CO_2, CH_4, and H_2) concentrations are measured by the gas analyzer, so the total molar flow rate, f_{out}, is calculated by the N_2 mass flow rate introduced:

$$f_{out} = \frac{f_{N_2}}{1 - \sum X_i} \tag{1}$$

where X_i (i = CO, CO_2, CH_4, and H_2) is the molar fraction of CO, CO_2, CH_4, and H_2 in the outlet gas flow.

The relative fraction of each component, W_i (i = CO, CO_2, CH_4, and H_2) is defined by the molar fraction of the flow of CO/CO_2/CH_4/H_2 in the product gas.

$$W_i = \frac{\int_0^t f_{out} \cdot X_i \cdot dt}{\int_0^t f_{out} \cdot (X_{CO} + X_{CO_2} + X_{CH_4} + X_{H_2}) \cdot dt} \tag{2}$$

The generation rate of gas including CO, CO_2, CH_4, and H_2, θ_i, is defined by the yield of each component per gram of petroleum coke:

$$\theta_i = \frac{\int_0^t f_{out} \cdot X_i \cdot dt}{m} \tag{3}$$

where m is the weight of petroleum coke adding in the reactor.

The carbon conversion efficiency, η_C, is the ratio of carbon consumed to the total carbon in the fuel and is computed by dividing the molar content of carbonaceous gas in the flue by the total molar content of carbon added into the reactor:

$$\eta_C = \frac{\int_0^t f_{out} \cdot (X_{CO} + X_{CO_2} + X_{CH_4}) \cdot dt}{n_{C,Fuel}} \times 100\% \tag{4}$$

where $n_{C,Fuel}$ is the molar content of carbon contained in the fuel.

The amount of substance in H_2S or SO_2, n_s(s = H_2S and SO_2), is defined by:

$$n_s = \int_0^t V_{out} \cdot Y_s \cdot dt \tag{5}$$

where Y_s(s = H_2S and SO_2) is the concentration of sulfur-containing gas.

3. Results and discussion

It is the first time to utilize petroleum coke by CLG process. It was meaningful to study the differences of the carbon and sulfur conversion between traditional steam gasification and CLG. Moreover, it was essential to evaluate the effect of different operating conditions on the performance of the petroleum coke, such as temperature, the flow rate of steam and the material size during CLG process.

3.1. Steam gasification and chemical looping gasification

Steam gasification was conducted using quartz sand as bed material in the same condition for comparison, to evaluate the effect of iron ore oxygen carriers on the gas releasing, carbon conversion efficiency and sulfur emission in the CLG process at 900 °C. The size of bed materials is 0.2–0.3 mm, and that of fuel is 0.1–0.3 mm. Fig. 4 shows the gas concentrations after water condensation during steam gasification and chemical looping gasification, respectively. As shown in Fig. 4(a), the petroleum coke gasification was intense in the first minute. The concentrations of H_2 and CH_4 reached maximum of 5.9% and 2.24%, and then decreased rapidly. The H_2 concentration fluctuated around 2%, and CH_4 decreased to zero. The first peak concentrations of CO and CO_2 were 0.65% and 0.32%, followed by another slight increase. The concentrations of H_2, CO and CO_2 were still 1.50%, 0.70% and 0.27% at 60th minute, indicating that the reactions were not completed within 60 min. The process could be divided to two parts: the devolatilization reaction with high reaction rate and the char gasification with rather low rate.

As shown in Fig. 4(b), the trends of the concentration of H_2, CH_4, CO_2 and CO in petroleum coke CLG process were similar to those observed in the steam gasification. But the maximum concentrations of each component were dramatically different with those in

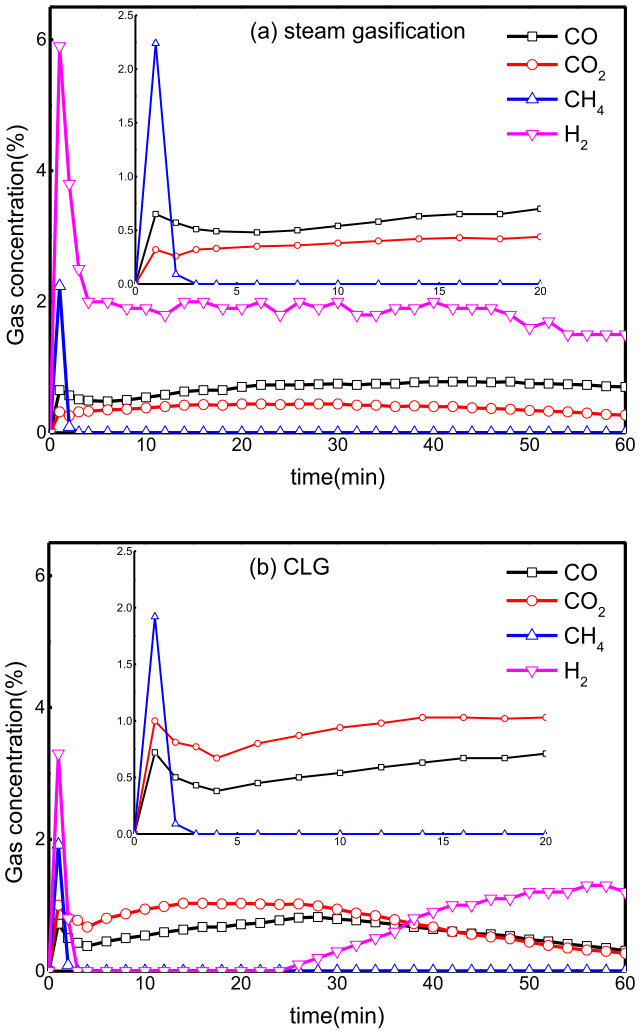

Fig. 4. Gas concentration during traditional steam gasification (a) and chemical looping gasification (b) at the fuel size of 0.1–0.3 mm and the bed material size of 0.2–0.3 mm at 900 °C.

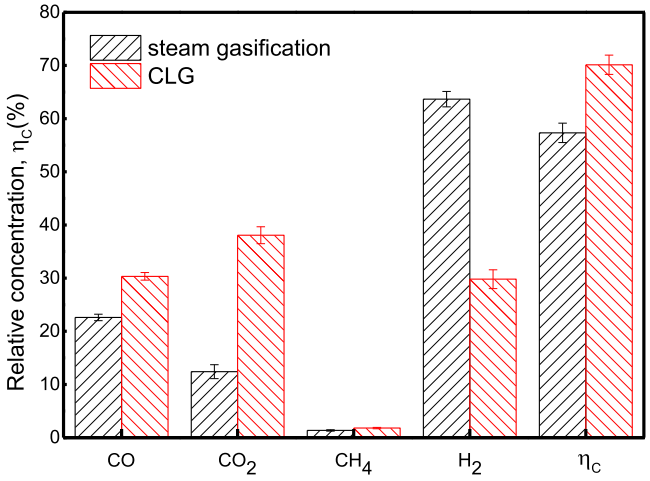

Fig. 5. Relative concentrations of outlet gas and carbon conversion efficiency during the steam gasification and CLG process.

the steam gasification process. The concentration of H_2 during the CLG process was much lower than that using quartz sand as bed material, and then it declined to zero quickly. It was interestingly noted that H_2 was observed after 24 min again. It may be ascribed to the insufficient hematite in the later process. There were two peaks for CO and CO_2 concentrations. The max concentrations of CO and CO_2 during the volatile releasing increased to 0.72% and 1.00%, in accord with the findings that oxygen carrier improved the generation of CO and CO_2 by Guo [12]. In the rest of the process, the maximum CO and CO_2 concentrations in the CLG process were 0.82% and 1.03%, higher than those in the steam gasification. It indicated that the oxygen carriers improved the conversion of char in petroleum coke.

Fig. 5 shows the relative concentrations of the outlet gas and carbon conversion efficiency during the steam gasification and CLG process within 60 min. The main component in the steam gasification were H_2 and CO, in accord with Wu's results [32]. But the H_2 concentration was lower than our results, because the steam gasification did not consist of the pyrolysis process in which a large amount of H_2 generated. In our work, H_2 accounted for 63.66% in steam gasification, while it decreased to 29.80% in the CLG process. A large portion of hydrogen was inevitably consumed by oxygen carrier. The relative fraction of CO_2 increased from 11.39% in the steam gasification to 38.08%, and CO_2 was the major product in the outlet gas in the CLG process. The carbon conversion efficiency reached 57.33% and 70.13% for the quartz sand and iron ore as bed materials, respectively. Furthermore, it just took 90 min to complete the conversion of fuel until the concentrations of gases declined to zero in CLG process, while it took 114 min in the steam gasification. So the oxygen carrier reduced the reaction time. These results manifested that the presence of iron ore as oxygen carriers enhanced the carbon conversion in the petroleum coke.

The differences between the traditional gasification and CLG mostly depended on the respective reactions. During the steam gasification, the main reactions involve the de-volatilization (R1) and those between steam and char in the petroleum coke (R2-R5). During the petroleum coke CLG based on iron ore, there are some simultaneous reactions between the oxygen carriers and the syngas as shown in (R6-R11) besides the reactions mentioned above. The lattice oxygen supplied by iron ore reacts with the gaseous products (primarily H_2, CO, CH_4) to generate CO_2 and H_2O. It was the reason why the relative fraction of H_2 decreased and CO_2 increased conversely. Thus, the syngas content was 61.92% in the CLG process, lower than that measured in steam gasification. The consumption of CO and H_2 improved the char gasification and further increase the carbon conversion. It had been reported that the reaction rate of H_2 was higher than that of CO as fuel to reduce the oxygen carrier [33]. So, compared with the case in steam gasification, the concentration of H_2 in CLG was lower, while the concentration of CO was slightly higher combining with the improvement of fuel conversion during the CLG process. Interestingly, we detected hydrogen again after the concentration became zero. The reductive iron may have catalytic effects on the char gasification and the water-gas-shift reaction. As the iron oxides phases in the atmosphere of CO/CO_2 and H_2/H_2O shown in Fig. 6, FeO exists when the ratio of $CO/(CO + CO_2)$ is in the range of 23–64% and $H_2/(H_2+H_2O)$ in the range of 31–61% at 900 °C [19]. The reactions during the process were complex. Therefore, Fe_3O_4 and FeO were the main forms of iron oxides during the reactions in the reactor. With the reactions in process, the amount of FeO would be accumulated. According to the reaction $H_2O+3FeO = Fe_3O_4+H_2$, hydrogen was generated at the atmosphere of excess steam. Moreover, the deep reduction to FeO or Fe is extremely difficult, so hydrogen may be residual and not converted to H_2O. In light of the changes of H_2 concentration, the whole CLG process composes of three periods:

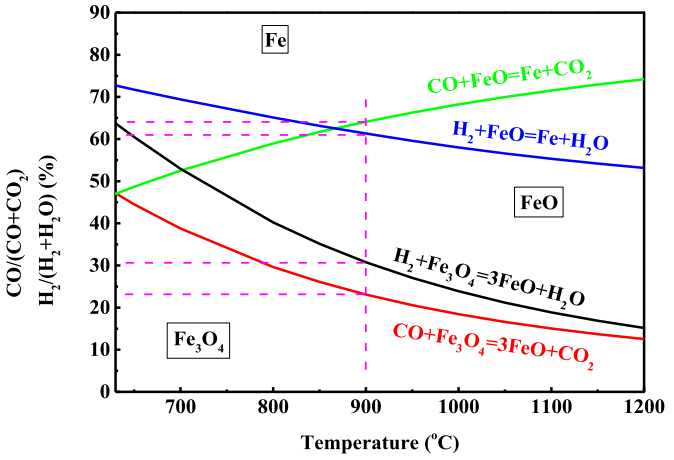

Fig. 6. Baur-Glaessner phase diagram of Fe oxides in the atmosphere of CO/CO_2 and H_2/H_2O.

the volatile releasing, the char gasification coupled with the oxidation of syngas and oxygen carriers, and the partial oxidation of reductive iron.

$$\text{Petroleum coke} \rightarrow \text{char} + \text{volatile} \quad \text{(R1)}$$

$$C\,(\text{char}) + H_2O \leftrightarrow CO + H_2 \quad \text{(R2)}$$

$$C\,(\text{char}) + CO_2 \leftrightarrow 2CO \quad \text{(R3)}$$

$$CH_4 + H_2O \leftrightarrow CO + 3H_2 \quad \text{(R4)}$$

$$CO + H_2O \leftrightarrow CO_2 + H_2 \quad \text{(R5)}$$

$$H_2 + 3Fe_2O_3 \rightarrow 2Fe_3O_4 + H_2O \quad \text{(R6)}$$

$$CO + 3Fe_2O_3 \rightarrow 2Fe_3O_4 + CO_2 \quad \text{(R7)}$$

$$CH_4 + 12Fe_2O_3 \rightarrow 8Fe_3O_4 + CO_2 + 2H_2O \quad \text{(R8)}$$

$$H_2 + Fe_3O_4 \leftrightarrow 3FeO + H_2O \quad \text{(R9)}$$

$$CO + Fe_3O_4 \leftrightarrow 3FeO + CO_2 \quad \text{(R10)}$$

$$CH_4 + 4Fe_3O_4 \leftrightarrow 12FeO + CO_2 + 2H_2O \quad \text{(R11)}$$

The reaction characteristics of petroleum coke are unique and different from coal and biomass, although the CO_2 concentration increased in the presence of oxygen carrier no matter what fuel is used. Guo [11] evaluated the CLG performance of Beisu bituminous coal based on Fe_2O_3 and found the CO_2 concentration had two peaks, but the second one was much lower than the first one. Ge [19] reported that there was only one peak for CO_2, but two peaks for CO, and the first CO peak was rather high compared to the second during the biomass CLG experiments. However, when petroleum coke was chosen as fuel, the tendencies of CO and CO_2 both had two peaks, and there were not great disparities between the two peak values, shown in Fig. 4(b). The coal and biomass mentioned above had 38.27%, 65.07% of volatile and 53.55%, 16.13% of fixed carbon. The petroleum coke has much more fixed carbon of 85.87% and less volatile of 12.98%. It can be explained by the larger amount of fixed carbon and smaller amount of volatiles in petroleum coke than that in coal and biomass. In addition, the fixed carbon was quite difficult to react in contrast to volatiles.

Fig. 7 displays the concentration changes of sulfur-containing gases (primarily H_2S and SO_2) during the steam gasification and CLG process within 2000 s at 900 °C. And to distinctly check the differences, the curves were enlarged for the initial 60 s. During the steam gasification, SO_2 was just detected in the first 30 s due to the volatile releasing from petroleum coke, while H_2S could be observed in the whole process. The concentrations of SO_2 and H_2S reached the maximum of 119 ppm and 916 ppm, respectively. The H_2S concentration sharply decreased to approximately 200 ppm and kept decreasing with a slower rate. Subsequently, it had a slight rise. H_2S was the main sulfur-containing component in steam gasification process. When iron ore was used as bed material, the maximum concentrations of SO_2 and H_2S were 1355 ppm and 428 ppm. Both of the H_2S and SO_2 concentrations appeared two peaks, and one was narrow and thin for the initial stage, while another was broad and lower than the first one. The second peak of SO_2 concentration was 141 ppm. Unlike steam gasification, SO_2 was the dominant component from the sulfur of petroleum coke in CLG process in the current case. The sum of SO_2 and H_2S concentrations during CLG was higher than that during steam gasification. The results indicated that iron ore improved not only the conversion of carbon but also the conversion of sulfur.

Besides the volatile sulfur releasing, H_2S also existed in the rest of the steam gasification process as a result of the gasification of sulfur in the char of petroleum coke. The form of sulfur is divided to organic and inorganic including pyritic and sulphate sulfur. Organic sulfur may interact with H in fuel releasing H_2S [34]. When the atmosphere is in H_2 during steam gasification, most sulfur is hydrogenated to H_2S according to R12 [35]. Pyritic sulfur, mainly Fe_2S, and then it was decomposed to $Fe_{(1-x)}S$. H_2S was the product of the gasification of steam and $Fe_{(1-x)}S$, according to R13. When using iron ore as bed material, the formation of H_2S in the CLG process was similar to that in the steam process, with two peaks, due to the volatile sulfur releasing and the gasification of sulfur mentioned above. The gasification product of sulfur H_2S was oxidized to SO_2 by the oxygen carriers as shown in R14 and R15. That can explain the occurrence of the second peak of SO_2 concentration and the transformation of dominant component from H_2S to SO_2. In addition, the major product CO_2 in the CLG process is an active oxidizing agent to improve the SO_2 generation from H_2S [36]. Therefore, SO_2 was the dominant sulfur form in CLG process. Furthermore, the presence of SO_2 had a positive influence on the gasification reactions of solid fuels [37,38]. Compared with steam gasification, the higher amount of SO_2 releasing was another reason for the enhancement of carbon conversion in the chemical looping

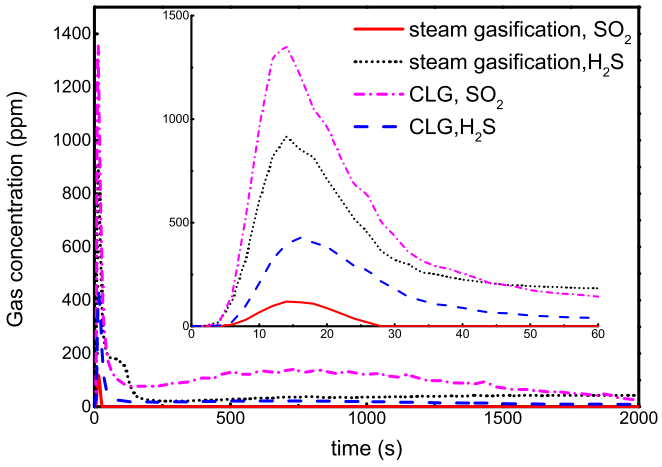

Fig. 7. Sulfur conversion during steam gasification and CLG process at 900 °C.

gasification.

$$S + H_2 \rightarrow H_2S \quad (R12)$$

$$Fe_{(1-x)}S + H_2O \rightarrow Fe_3O_4/FeO + H_2S \quad (R13)$$

$$9Fe_2O_3 + H_2S \rightarrow 6Fe_3O_4 + SO_2 + H_2O \quad (R14)$$

$$3Fe_3O_4 + H_2S \rightarrow 9FeO + SO_2 + H_2O \quad (R15)$$

3.2. Effect of reaction temperature on the carbon and sulfur conversion in the CLG process

Experiments were carried out where the temperature was set to 850, 900, and 950 °C. And the size of iron ore was 0.2–0.3 mm and petroleum coke was 0.1–0.3 mm when using steam as gasification agent at a rate of 1 g/min. Fig. 8 displays the generation rates of CO, CO_2, CH_4 and H_2 as a function of temperature during the reduction period. Except for CH_4 which did not have significant difference, the generation rates of CO, CO_2, and H_2 increased with the temperature in the range of 850–950 °C. The increasing generation rates of those component from 850 °C to 900 °C were dramatic, whereas those increasing rates declined from 900 °C to 950 °C. The H_2 yield increased seven times in the first interval of 50 °C, and just continued increasing by less than 10% in the next temperature interval. Similarly, the CO yield first increased by 66%, and then the increase slowed down to 2%. The decline of the increasing rate of CO_2 yield from the first 50 °C to the second 50 °C was not as significant as those of CO and H_2. Those results indicated that the increasing temperature from 850 °C to 900 °C mainly affected the petroleum coke conversion, and the temperature from 900 °C to 950 °C led to the reactivity improvement of oxygen carrier. The gasification of char (R2) was endothermic, favored by the increasing temperature. Thus, the yields of CO and H_2 were enhanced. Additionally, the increasing temperature enhanced the reductive reactivity of iron ore (R6-7, R9-10), resulting in generating more CO_2 and H_2O with the consumption of CO and H_2 in the second interval of 50 °C. In terms of the yield, CO was the dominant component at 850 °C, but CO_2 took the place of CO at 900 and 950 °C.

Fig. 9 shows the carbon conversion efficiency together with the sum of molar fractions of CO, H_2, and CH_4 at different temperatures.

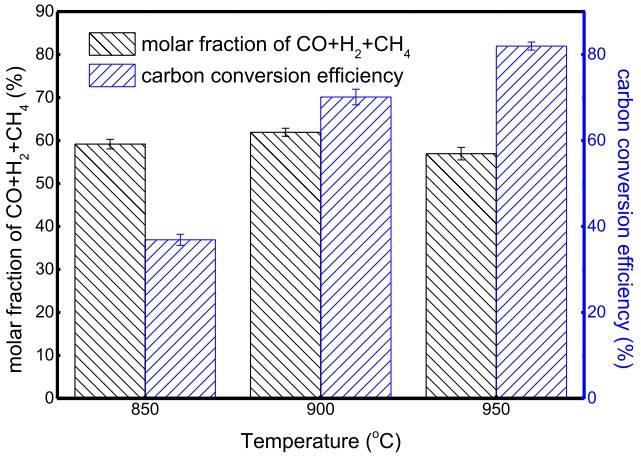

Fig. 9. Effect of temperature on the molar fraction of syngas and carbon conversion.

The carbon efficiency increased from 36.91% at 850 °C to 70.13% at 900 °C and 81.98% at 950 °C, respectively. However, after the slight rise in the sum of molar fractions of flammable gases, the molar fraction had a drop when the temperature continued increasing to 950 °C. The molar fraction of syngas and the carbon conversion efficiency also exhibited increasing tendency with temperature from 750 °C to 900 °C in the CLG process with biomass [19]. Although the high temperature accelerated the conversion of petroleum coke, the additional part of CO, H_2, and CH_4 was consumed by the lattice oxygen from iron ore because the reactivity of oxygen carriers was promoted by the increasing temperature. The results verified the inferences that the limited factor was the gasification of petroleum coke at the temperature below 900 °C, while the temperature above 900 °C brought more impact on the reactivity of oxygen carriers.

Fig. 10 presents the effect of temperature on the average concentration of SO_2 and H_2S during the reduction period of CLG process. The average of SO_2 concentration at 900 °C was as 2.6 times as that at 850 °C. At 950 °C, the SO_2 concentration was 5% more than that at 900 °C. It was obvious that the SO_2 concentration increased with the increasing temperature, and it reached 110.55 ppm at 950 °C. In light of the H_2S concentration, it was highest at 900 °C. The H_2S concentration declined slightly when the temperature was up to 950 °C because R13 and R14 were

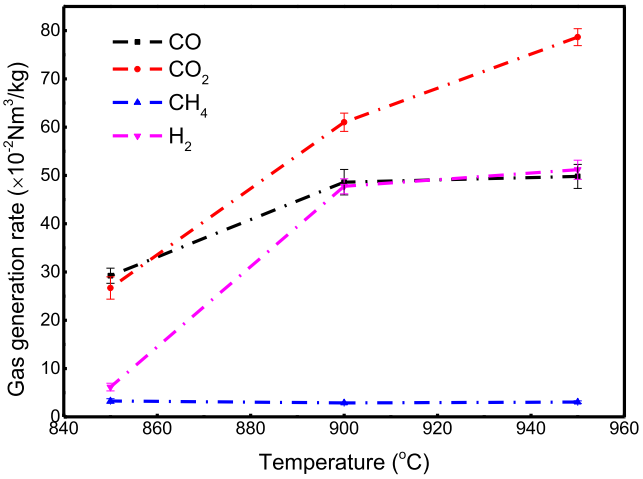

Fig. 8. Effect of temperature on the generation rates of outlet gases in the CLG process.

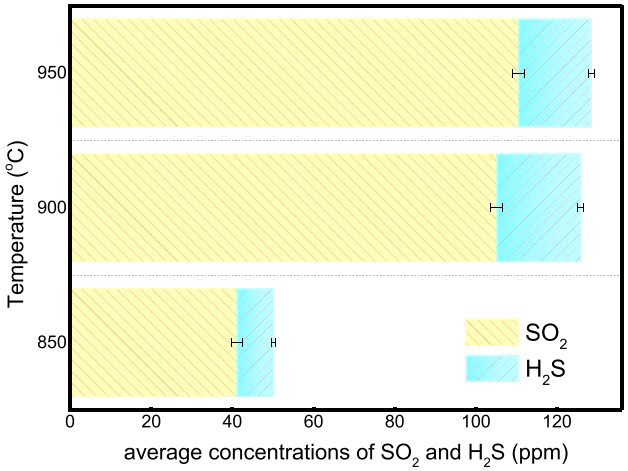

Fig. 10. Effect of temperature on the sulfur conversion.

endothermic reactions. Moreover, the oxygen carriers exhibited better reactivity at the higher temperature. More H_2S was oxidized to SO_2, thus the amount of H_2S decreased. The significant increase of the sum of average concentrations of SO_2 and H_2S from 850 °C to 900 °C was ascribed to the enhancement of the char gasification of petroleum coke. When the temperature was set to more than 900 °C, the sum of sulfur gases maintained increasing but the increase extent was smaller.

3.3. Effect of steam flow rate on the carbon and sulfur conversion in the CLG process

Fig. 11 displays the generation rates of each component (CO, CO_2, CH_4 and H_2) during the reduction period when the flow rate of steam was 0.5, 1, and 1.5 g/min as gasification agent, respectively. The CH_4 generation rate was the lowest among the outlet gases measured, and it fluctuated between 0.0283 and 0.0356 Nm^3/kg. The CO_2 generation rate kept steady and stable growth with the increasing flow rate of steam. H_2 visibly increased by 0.3183 Nm^3/kg as the steam flow rate increased from 0.5 g/min to 1 g/min, and continued slightly increasing to 0.5287 Nm^3/kg at the steam flow rate of 1.5 g/min. The increasing H_2 and CO_2 yields with steam flow rate were consistent with the performance of biomass in the CLG process [19]. The generation rate of H_2 largely depended on the amount of steam injected into the reactor. The high flow rate of steam not only improved the difficult gasification of petroleum coke, but also reduced the residence time of hydrogen which reacted with oxygen carrier. The steam flow rate of 0.5 g/min was not sufficient for petroleum coke gasification. On the contrary, the CO generation rate decreased when the steam flow rate increased from 1 g/min to 1.5 g/min. The excessive concentration of steam strengthened the positive reactions of R2 and R5, which resulted in a decrease of CO, and increases of H_2 and CO_2.

The sum of molar fractions of syngas at different flow rate of steam is shown in Fig. 12 along with the carbon conversion efficiency. The carbon conversion efficiency increased by 6.45% at steam flow rate of 1 g/min, and 9.93% at that of 1.5 g/min, as compared with the case at steam flow rate of 0.5 g/min. When the flow rate of steam rose from 0.5 to 1 g/min, the sum of molar fractions of effective gases (CO, H_2 and CH_4) increased from 56.09% to 61.92%. Instead, there was not a visible increase when the steam flow rate continued increasing to 1.5 g/min. The reason for this was most likely explained by the comprehensive consequence of the

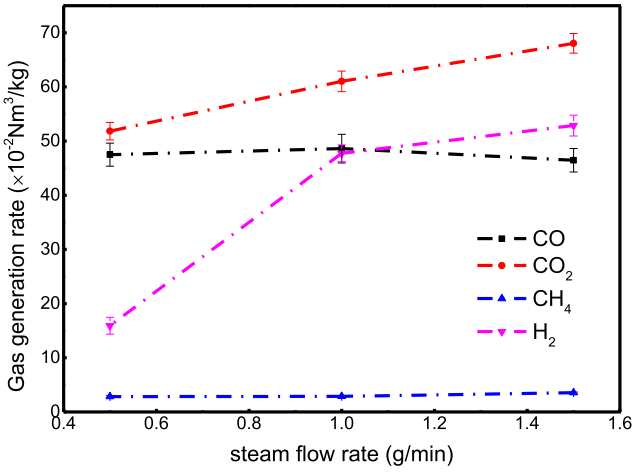

Fig. 11. Effect of steam flow rate on the generation rates of outlet gases in the CLG process.

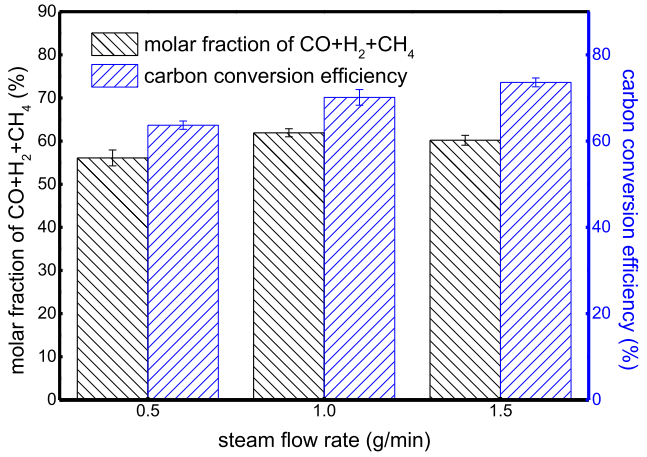

Fig. 12. Effect of steam flow rate on the molar fraction of syngas and carbon conversion.

improvement of gasification of char in the petroleum coke and the increasing yield of CO_2 from the water-gas shift reaction (R5). Therefore, 1 g/min was the suitable flow rate of steam for the CLG process based on iron ore with petroleum coke as fuel in this work.

The different flow rates of steam made the volumes of outlet gases significantly different. It was more reasonable to describe the distribution of H_2S and SO_2 via the amounts of substance in them and the molar fraction of H_2S to SO_2 during the CLG process at different steam flow rate, as shown in Fig. 13. The amounts of substance in H_2S and SO_2 increased with the increasing flow rate of steam, but the molar fraction of H_2S to SO_2 was around 0.2, which was not greatly influenced by the amount of steam. The flow rate of steam improved the gasification of sulfur and carbon in the char of petroleum coke in the CLG process. Sequentially, the gasification product H_2S was oxidized to SO_2, so the sum amount of substance of sulfur-containing gases increased. However, the flow rate of steam had weak effect on the molar fraction of H_2S to SO_2.

3.4. Effect of material size on the carbon and sulfur conversion in the CLG process

3.4.1. Effect of the size of petroleum coke particles

Fig. 14(a) displays the main components of conventional gas and

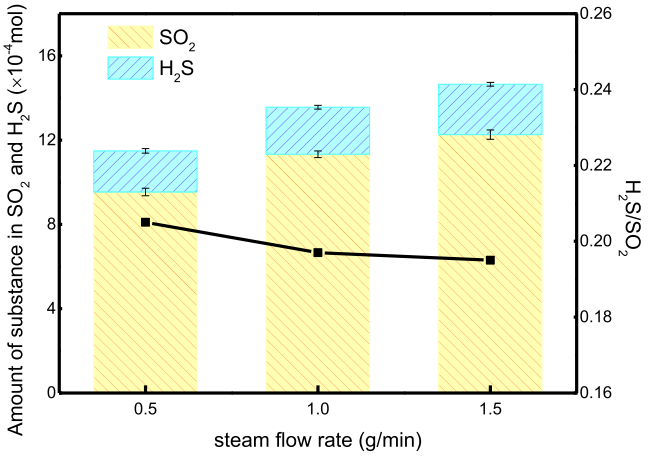

Fig. 13. Effect of steam flow rate on the sulfur conversion.

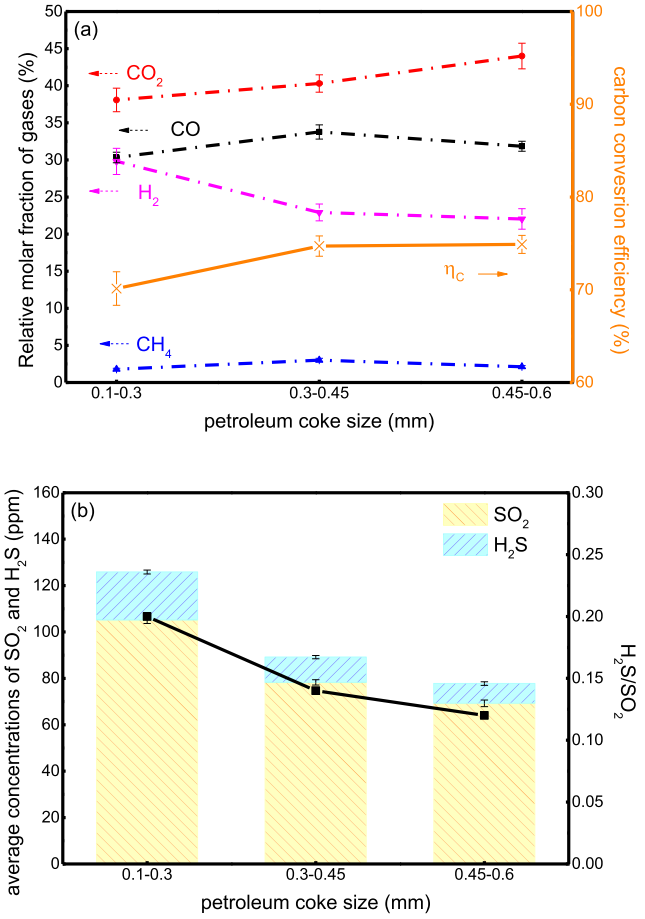

Fig. 14. Effect of the size of petroleum coke particles on (a) carbon conversion and (b) sulfur conversion.

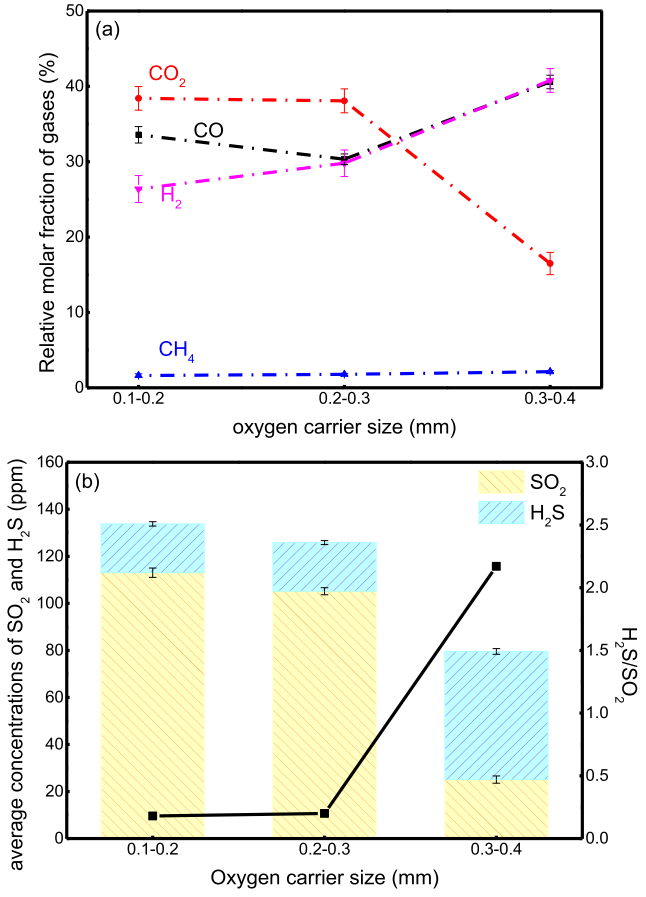

Fig. 15. Gas releasing during the CLG process with different sizes of oxygen carrier (a) conventional gases (b) sulfur-containing gases.

the carbon conversion efficiency when the size of hematite was 0.2–0.3 mm and that of petroleum coke was respectively 0.1–0.3 mm, 0.3–0.45 mm, and 0.45–0.6 mm within 60 min during the reduction period. The CO_2 concentration increased steadily as the size of petroleum coke enlarged. Instead, the H_2 concentration decreased. The trends of CO and CH_4 presented an apparent increase following with a decline. The gasification of the small size of petroleum coke was faster. The increasing yields of gases made the residence time shorter and the gas-solid contact worse. The rest of unreacted H_2 was much more. Similarly, the slow gasification rate of the fuel particles in a large size was the reason of the opposite tendency of CO and CO_2 in comparison with those in medium size. The gasification rate was much slower than the oxidization rate with oxygen carrier. A large size led to an increase in carbon conversion efficiency from 70% to 75%. The average concentrations of SO_2 and H_2S with different fuel sizes within 2000 s are presented in Fig. 14(b), as well as the molar ratio of H_2S to SO_2. With the increasing size of fuel, not only the concentration of SO_2 but also that of H_2S decreased, though the decreasing magnitude was reducing. The larger size of fuel had contributed to a low conversion of sulfur. Moreover, the molar fraction of H_2S to SO_2 also decreased with the increasing size of fuel, and it was always less than 2.

3.4.2. *Effect of the size of oxygen carrier particles*

Fig. 15(a) displays the gases releasing within 60 min during the CLG process using different sizes of hematite of 0.1–0.2 mm, 0.2–0.3 mm and 0.3–0.4 mm when the size of petroleum coke was 0.1–0.3 mm. When the hematite size was 0.1–0.2 mm or 0.2–0.3 mm, the main component was CO_2, accounting for approximately 38%. However, the major constituents were CO and H_2 rather than CO_2 when the oxygen carrier size was 0.3–0.4 mm. CO accounted for 40.6% and H_2 accounted for 40.8%. The larger size of oxygen carrier was conducive to the production of effective syngas. The oxygen carrier size of 0.3–0.4 mm was appropriate for the carbon conversion during the CLG process. Fig. 15(b) presents the molar fraction of H_2S/SO_2, and the average concentrations of SO_2 and H_2S within 2000s using the hematite oxygen carrier in the small, medium and large size. The sum concentrations of SO_2 and H_2S, as well as the average concentration of SO_2, decreased with the increasing size of oxygen carrier. As compared to the case with hematite oxygen carrier in small and medium size, the distribution of sulfur-containing gas had changed when oxygen carrier was used in a large size, because the hematite particles in large size provided a small amount of lattice oxygen. The decreasing concentration of CO_2 is another reason for the decline of SO_2 and rise in H_2S [35,36]. The molar fraction of H_2S/SO_2 was 0.2 when the oxygen carrier size was 0.1–0.2 mm. And the molar fraction was about 2 when the size was 0.3–0.4 mm, which met the requirement of the Claus process for sulfur recovery. Therefore, the suitable size of hematite oxygen carrier particles was 0.3–0.4 mm for the effective syngas production and sulfur recovery during the chemical looping gasification based on petroleum coke in this work.

The Claus process was the most widely employed and mature technology for sulfur removal and recovery from gaseous H_2S and SO_2. It was first proposed in 1883, according to R15 [39,40]. And

I.G.Farben improved the process to a two-step oxidation [41]. In the first thermal step, hydrogen sulfide in the stream is burnt to form SO_2 using air, as shown in R16. The product further undergoes Claus reaction between H_2S and SO_2 like R17. In addition, the unreacted H_2S reacts with SO_2 to form elemental sulfur in fixed bed reactors in the catalytic step. The reaction is the same as R17 [42,43]. In the chemical looping gasification process, the oxygen carrier provides lattice oxygen to take place of the oxygen from air. If the molar fraction of H_2S/SO_2 is 2, the mixture stream can be introduced in the Claus plants directly for sulfur recovery simplifying processes. In this way, petroleum coke was used to produce syngas and recover sulfur based on chemical looping gasification technology. The molar fraction of H_2S/SO_2 can be adjusted by changing the reaction conditions. It achieved the requirement, when the petroleum coke size was 0.1–0.3 mm and the hematite oxygen carrier was 0.3–0.4 mm at 900 °C, which was optimum in the work.

$$H_2S + 0.5O_2 \rightarrow (1/n)S_n + H_2O \quad \text{(R15)}$$

$$2H_2S + 3O_2 \rightarrow 2SO_2 + 2H_2O \quad \text{(R16)}$$

$$2H_2S + SO_2 \rightarrow (3/n)S_n + 2H_2O \quad \text{(R17)}$$

The fuel gas, electricity and deoxidized water were the top energy consumption in the Claus processes. Simultaneously, the Clause processes also produced energy including steam and sulfur. If the molar fraction of H_2S to SO_2 is 2 in the flue gas of CLG process, the combustion furnace could be omitted. The steam required as gasification agent can be provided by the condensation of H_2O in the flue gas or the high-pressure steam from waste heat boil. And the gas required for CLG process could be preheated by the high-temperature steam to recycle heat. Moreover, oxygen was provided by oxygen carrier in CLG process, so the energy consumption of air separators reduced. In addition, the presence of oxygen carrier improved the carbon conversion efficiency, and the petroleum coke consumption decreased, as compared with the traditional steam gasification. In conclusion, the integration of CLG and Claus processes exhibits high energy efficiency and low energy consumption with good environmentally friendly and economic performance.

3.5. Characterization of oxygen carriers

Gu [44] had found that the sulfuration of iron-ore oxygen carrier happened during the chemical looping combustion and resulted in an imperforate surface and a decrease in reactivity. Arabczyk [45] had also reported that iron catalyst was easily poisoned by sulfur. Special attention should be paid to the properties of hematite after the chemical looping process. Fig. 16 displays the surface morphology of the fresh and reacted hematite at low magnification (5000 ×) and high magnification (40000 ×), characterized by scanning electron microscope (SEM). The reacted oxygen carrier produced porous structure in yellow circles, while the surface of fresh oxygen carrier seemed to be dense. The number and size of pores increased significantly. For the reacted hematite, the sharp-edged particle margins were polished and disappeared as marked in green rectangles, but there was no obvious sintering. And Energy Dispersive X-ray Detector (EDX) was used to measure the elemental compositions on the surface of fresh and reacted oxygen carrier in the blue square. In Fig. 17, no element sulfur was detected on the surface, indicating that the sulfur in the petroleum coke did not stay on the hematite surface in the sulfur migration when chemical looping gasification proceeded. The oxygen carrier was not poisoned by the high sulfur petroleum coke. The main components

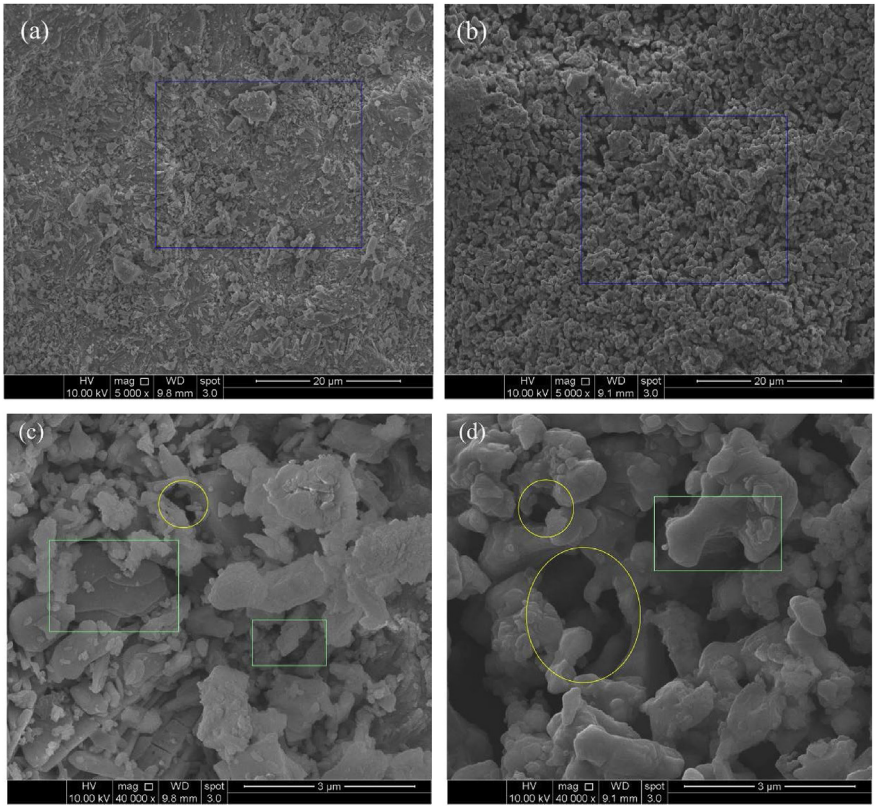

Fig. 16. SEM images of (a,c) fresh and (b,d) reacted hematite.

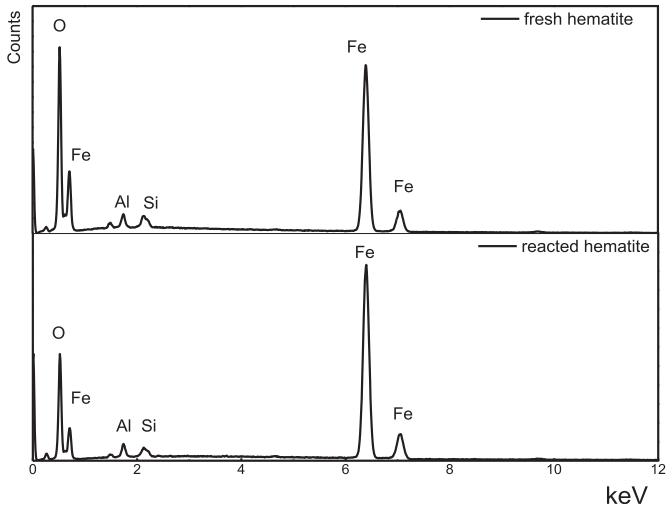

Fig. 17. EDX analysis of fresh and reacted hematite.

in the reacted hematite were Fe, O, Al and Si, which were the same as the fresh hematite. The EDX results of the atomic weight fraction were summarized in Table 5. The weight fraction of Fe to O increased to 3.4, between 2.6 and 3.5, so it was suggested that the forms of Fe were Fe_3O_4 and FeO after the reduction stage.

4. Conclusion

Chemical looping gasification with hematite is an attractive and alternative method for high-sulfur petroleum coke conversion and sulfur recovery via Claus reaction due to its high heating value, low ash content and high sulfur content. Hematite is regarded as oxidant to provide lattice oxygen for gasification and the first step of Claus process. Experiments were conducted in a batch fluidized bed to evaluate the feasibility and performance of petroleum coke chemical looping gasification. The main conclusion are as follows:

The presence of hematite oxygen carrier had an effect on the gas releasing distribution. CO_2 and SO_2 replace H_2 and H_2S to be the main product in the CLG process. Although the molar fraction of syngas decreased inevitably, the carbon conversion efficiency increased by 12.8%. And the sulfur conversion was improved. Unlike the two stages of conventional steam gasification, the CLG process can be divided to three parts: the rapid volatile releasing, the slow char gasification coupled with the oxidation of syngas and oxygen carriers, and the partial oxidation of reductive iron in light of the trend of H_2 concentration.

The increasing temperature contributes to the conversion of carbon and sulfur. The generation rates of gases increased as the temperature raised, especially CO_2. However, the steam flow rate had a complex effect on the generation rates of different gas. The molar fraction of the effective syngas reached 61.92% when the temperature was 900 °C at a steam flow rate of 1 g/min. Considering about the slow gasification reactions and the distribution of SO_2 and H_2S, the sizes of petroleum coke and hematite should be set to 0.1–0.3 mm and 0.3–0.4 mm, respectively. And the outlet stream with the molar fraction of H_2S/SO_2 of 2, could be directly used to produce element sulfur via Claus reaction.

Additionally, sulfur in the petroleum coke did not stay on the hematite surface in the sulfur migration of CLG process, indicating that the oxygen carrier was not poisoned by the high sulfur petroleum coke.

Table 5
Elemental compositions on the surface of fresh and reacted hematite (wt%).

	Fresh hematite	Reacted hematite
O	27.94	22.12
Fe	69.65	75.63
Al	0.88	0.79
Si	1.53	1.46
Fe/O	2.5	3.4

Acknowledgements

We gratefully acknowledge the support of this research work by the National Natural Science Foundation of China (Grant No. 51561125001) and the Postgraduate Research & Practice Innovation Program of Jiangsu Province (Grant No. KYCX18_0082).

Nomenclature

Abbreviations

CLG	Chemical looping gasification
CLC	Chemical looping combustion
XRF	X-ray Fluorescence
BET	Brunauer-Emmett-Teller
SEM	Scanning Electron Microscope
EDX	Energy Dispersive X-ray Detector

Notation list

f_{N_2}	inlet molar flow rate of N_2 [mol/min]
f_{out}	total molar flow rate of outlet [mol/min]
X_i	molar fraction of component i [−]
W_i	relative fraction of component i [−]
θ_i	generation rate of component i [Nm^3/g]
M	weight of petroleum coke [g]
η_C	carbon conversion efficiency [−]
$n_{C,Fuel}$	molar content of carbon in the fuel [mol]
n_s	amount of substance in H_2S or SO_2 [mol]
Y_s	concentration of H_2S or SO_2 [ppm]

References

[1] Wang J, Anthony EJ, Abanades JC. Clean and efficient use of petroleum coke for combustion and power generation. Fuel 2004;83:1341–8.
[2] Wang MR, Chang KC. Study on reduction of SO2 and NOX emissions in a pulsating combustor burning petroleum coke. Energy 1991;16:849–58. 1991/05/01/.
[3] Nemanova V, Abedini A, Liliedahl T, Engvall K. Co-gasification of petroleum coke and biomass. Fuel 2014;117:870–5.
[4] Zhou ZJ, Hu QJ, Liu X, Yu GS, Wang FC. Effect of iron species and calcium hydroxide on high-sulfur petroleum coke CO2 gasification. Energy Fuels 2012;26:1489–95.
[5] Zhan X, Jia J, Zhou Z, Wang F. Influence of blending methods on the co-gasification reactivity of petroleum coke and lignite. Energy Convers Manag 2011;52:1810–4.
[6] Wang G, Zhang J, Zhang G, Ning X, Li X, Liu Z, et al. Experimental and kinetic studies on co-gasification of petroleum coke and biomass char blends. Energy 2017;131:27–40. 2017/07/15/.
[7] Lee SH, Yoon SJ, Ra HW, Son YI, Hong JC, Lee JG. Gasification characteristics of coke and mixture with coal in an entrained-flow gasifier. Energy 2010;35:3239–44.
[8] Wu Y q, Wu S y, Gu J, Gao J s. Differences in physical properties and CO2 gasification reactivity between coal char and petroleum coke. Process Saf Environ Protect 2009;87:323–30.
[9] Zou J, Yang B, Gong K, Wu S, Zhou Z, Wang F, et al. Effect of mechanochemical treatment on petroleum coke–CO 2 gasification. Fuel 2008;87:622–7.
[10] Kun Z, He D, Guan J, Zhang Q. Thermodynamic analysis of chemical looping gasification coupled with lignite pyrolysis. Energy 2019;166:807–18. 2019/01/01/.
[11] Guo QJ, Cheng Y, Liu YZ, Jia WH, Ryu HJ. Coal chemical looping gasification for syngas generation using an iron-based oxygen carrier. Ind Eng Chem Res 2014;53:78–86.
[12] Guo QJ, Hu XD, Liu YZ, Jia WH, Yang MM, Wu M, et al. Coal chemical-looping

gasification of Ca-based oxygen carriers decorated by CaO. Powder Technol 2015;275:60–8.
[13] Zhan X, Zhou Z, Wang F. Catalytic effect of black liquor on the gasification reactivity of petroleum coke. Appl Energy 2010;87:1710–5.
[14] Wu Y, Wang J, Wu S, Huang S, Gao J. Potassium-catalyzed steam gasification of petroleum coke for H2 production: reactivity, selectivity and gas release. Fuel Process Technol. 2011;92:523–30.
[15] Zeng L, He F, Li F, Fan L-S. Coal-direct chemical looping gasification for hydrogen production: reactor modeling and process simulation. Energy Fuels 2012;26:3680–90.
[16] Udomsirichakorn J, Basu P, Salam PA, Acharya B. CaO-based chemical looping gasification of biomass for hydrogen-enriched gas production with in situ CO2 capture and tar reduction. Fuel Process Technol. 2014;127:7–12.
[17] Huang Z, He F, Feng Y, Liu R, Zhao K, Zheng A, et al. Characteristics of biomass gasification using chemical looping with iron ore as an oxygen carrier. Int J Hydrogen Energy 2013;38:14568–75.
[18] Huang Z, He F, Feng Y, Zhao K, Zheng A, Chang S, et al. Biomass char direct chemical looping gasification using NiO-modified iron ore as an oxygen carrier. Energy Fuels 2013;28:183–91.
[19] Ge HJ, Guo WJ, Shen LH, Song T, Xiao J. Experimental investigation on biomass gasification using chemical looping in a batch reactor and a continuous dual reactor. Chem Eng J. 2016;286:689–700.
[20] Adánez J, de Diego LF, García-Labiano F, Gayán P, Abad A, Palacios J. Selection of oxygen carriers for chemical-looping combustion. Energy Fuels 2004;18:371–7.
[21] Zafar Q, Mattisson T, Gevert B. Redox investigation of some oxides of transition-state metals Ni, Cu, Fe, and Mn supported on SiO 2 and MgAl 2 O 4. Energy Fuels 2005;20:34–44.
[22] Mattisson T, Järdnäs A, Lyngfelt A. Reactivity of some metal oxides supported on alumina with alternating methane and Oxygen Application for chemical-looping combustion. Energy Fuels 2003;17:643–51.
[23] Ge HJ, Guo WJ, Shen LH, Song T, Xiao J. Biomass gasification using chemical looping in a 25 kW th reactor with natural hematite as oxygen carrier. Chem Eng J. 2016;286:174–83.
[24] Leion H, Jerndal E, Steenari B-M, Hermansson S, Israelsson M, Jansson E, et al. Solid fuels in chemical-looping combustion using oxide scale and unprocessed iron ore as oxygen carriers. Fuel 2009;88:1945–54.
[25] Azargohar R, Gerspacher R, Dalai AK, Peng D-Y. Co-gasification of petroleum coke with lignite coal using fluidized bed gasifier. Fuel Process Technol. 2015;134:310–6.
[26] Gu H, Shen L, Xiao J, Zhang S, Song T, Chen D. Iron ore as oxygen carrier improved with potassium for chemical looping combustion of anthracite coal. Combust Flame 2012;159:2480–90.
[27] Ge H, Shen L, Gu H, Jiang S. Effect of co-precipitation and impregnation on K-decorated Fe2O3/Al2O3 oxygen carrier in Chemical Looping Combustion of bituminous coal. Chem Eng J. 2015;262:1065–76.
[28] Jiang S, Shen L, Wu J, Yan J, Song T. The investigations of hematite-CuO oxygen carrier in chemical looping combustion. Chem Eng J. 2017;317:132–42.
[29] Liu W, Shen L, Gu H, Wu L. Chemical looping hydrogen generation using potassium-modified iron ore as an oxygen carrier. Energy Fuels 2016;30:1756–63.
[30] Niu X, Shen L, Jiang S, Gu H, Xiao J. Combustion performance of sewage sludge in chemical looping combustion with bimetallic Cu–Fe oxygen carrier. Chem Eng J. 2016;294:185–92.
[31] Wang LL, Shen LH, Liu WD, Jiang SX. Chemical looping hydrogen generation using synthesized hematite-based oxygen carrier comodified by potassium and copper. Energy Fuels 2017;31:8423–33.
[32] Wu SY, Huang S, Wu YQ, Gao JS. The reactivity and H2Production characteristics of petroleum coke-steam gasification catalyzed by potassium salts. Energy Sources, Part A Recovery, Util Environ Eff. 2013;36:184–90.
[33] Chen YG, Galinsky N, Wang ZR, Li FX. Investigation of perovskite supported composite oxides for chemical looping conversion of syngas. Fuel 2014;134:521–30.
[34] Attar A, Corcoran WH. Desulfurization of organic sulfur compounds by selective oxidation. 1. Regenerable and nonregenerable oxygen carriers. Ind Eng Chem Prod Res Dev. 1978;17:102–9. 1978/06/01.
[35] Gu Y, Yperman J, Vandewijngaarden J, Reggers G, Carleer R. Organic and inorganic sulphur compounds releases from high-pyrite coal pyrolysis in H2, N2 and CO2: test case Chinese LZ coal. Fuel 2017;202:494–502. 2017/08/15/.
[36] Wang B, Yan R, Lee DH, Liang DT, Zheng Y, Zhao H, et al. Thermodynamic investigation of carbon deposition and sulfur evolution in chemical looping combustion with syngas. Energy Fuels 2008;22:1012–20. 2008/03/01.
[37] Leion H, Mattisson T, Lyngfelt A. The use of petroleum coke as fuel in chemical-looping combustion. Fuel 2007;86:1947–58.
[38] Lyon RK, Cole JA. Unmixed combustion: an alternative to fire. Combust Flame 2000;121:249–61.
[39] Piã‰plu Anne, Saur Odette, Lavalley Jean-Claude, Legendre Oliver, Nã‰dez Christophe. Claus catalysis and H2S selective oxidation. Catal Rev. 1998;40:409–50.
[40] Fischer H. Burner fire box design improves sulfur recovery. Hydrocarb Process 1974;53:125–30.
[41] Mahdipoor HR, Ganji H, Naderi H. Adjusting the furnace and converter temperature of the sulfur recovery units. 2012.
[42] Elsner MP, Menge M, Muller C, Agar DW. The Claus process: teaching an old dog new tricks. Catal Today Apr 2003;79:487–94.
[43] Mahdipoor HR. Effect of reaction furnace and converter temperatures on performance of sulfur recovery units (SRUs). Journal of Petroleum Science Research 2012;1:1–3.
[44] Gu H, Shen L, Xiao J, Zhang S, Song T, Chen D. Evaluation of the effect of sulfur on iron-ore oxygen carrier in chemical-looping combustion. Ind Eng Chem Res. 2013;52:1795–805.
[45] Arabczyk W, Moszyński D, Narkiewicz U, Pelka R, Podsiadły M. Poisoning of iron catalyst by sulfur. Catal Today 2007;124:43–8.